# Asymmetric supercapacitors fabricated with ferrite/CHTL-derived hydrochar electrodes

K. Huynh, B. Maddipudi, V.S.Amar, G.Bauer, A.Shende, and R.V.Shende*

Karen M. Swindler Department of Chemical and Biological Engineering,

South Dakota School of Mines & Technology

Rapid City, SD 57701 USA, *Rajesh.Shende@sdsmt.edu

## ABSTRACT

In this investigation, Mn-ferrite was synthesized using a sol-gel method and utilized as an electrode material with catalytic liquefaction (CHTL) derived hydrochar electrode to fabricate an asymmetric supercapacitor (ASC). To prepare Mn-ferrite, precursor salts of Mn and Fe were taken in ethanol and dispersed using sonication. To this dispersion, propylene oxide was added to achieve the gel formation. The gel was aged for 24 hours and calcined at different temperatures of 300°, 600° and 900°C for 5 hours. The powdered materials obtained after calcination were characterized with x-ray diffraction (XRD) to investigate phase composition. Mn-ferrite and KOH activated hydrochar were used as electrodes for ASCs, which were tested by cyclic voltammetry (CV) to determine the specific capacitance.

***Keywords:*** Mn-ferrite, sol-gel, asymmetric supercapacitor, hydrochar, porous carbon (POC)

## 1 INTRODUCTION

Electrical energy storage systems are currently being used in a variety of applications such as portable devices, electric vehicles, consumer appliances and more [1]. Among the energy storage systems (e.g. batteries or capacitors/supercapacitors), asymmetric supercapacitors (ASCs) have gained much attention because of their longer cyclic stability as compared to batteries/capacitors and higher energy/power densities as compared to electric double-layer capacitors (EDLCs) [2,3]. ASCs refer to the devices with dissimilar electrode materials in which the charge storage mechanism is satisfied by the Faradic reaction between the electrode materials and electrolyte [4]. Due to the nature of the charge storage mechanism in ASC, its performance is highly dependent on the electrode material.

Electrode materials such as transition metal oxides- $RuO_2$, $IrO_2$, $WO_3$, $MnO_2$, $Mn_3O_4$ etc. and different carbon materials have been investigated for ASC [5,6]. In addition, spinel ferrites (e.g., $NiFe_2O_4$, $MnFe_2O_4$, $ZnFe_2O_4$) have been studied as electrode materials for ASCs due to their great thermal stability and rich redox chemistry [7]. With mixed metal oxides or ferrite electrodes, carbon-based materials such as graphene, graphene oxide, carbon nanotubes, and hydrochar were explored as negative electrode because of their higher electric conductivity as well as specific surface area (SSA) [8]. Askari et.al. used $NiFe_2O_4$ and reduced graphene oxide electrodes for ASC and reported a maximum capacitance of 584.63 F/g and capacitance retention of 91% after 2000 cycles [9]. Fu et.al. used $MnFe_2O_4$ with graphene and reported a specific capacitance of 537.7 F/g at current density of 0.5 A/g [10]. These results indicate the potential of ferrite materials for ASCs. Industrially carbon materials are derived from fossil fuels, which are known to contribute to the greenhouse gas (GHG) emission. Alternatively, carbons valorized from lignocellulosic biomass (LCB) feedstocks will be more sustainable with less impact on environment.

Recently, our group reported performance of the ASCs fabricated using POC derived from corn stover and sol-gel derived (Mn, Ti)-oxides. An average specific capacitance of 92.3 F/g was observed for the ASC prepared with POC/(Mn, Ti)-oxides (calcined as heating to 500°C, cooling to room temperature, followed by heating to 1000°C and cooling) [11].

In this investigation, ASCs were fabricated using sol-gel derived $MnFe_2O_4$ and KOH activated CHTL-derived hydrochar and their performance was measured using cyclic voltammetry.

## 2 EXPERIMENTAL

### 2.1 Materials

Manganese (II) chloride tetrahydrate ($MnCl_2.4H_2O$, MW=197.91, 99%, Arcos Organics, NJ) and iron (II) chloride tetrahydrate ($FeCl_2.4H_2O$, MW=198.81, 98%, Alfa Aesar, MA) were used for the sol-gel synthesis of $MnFe_2O_4$. Ethanol (200 Proof) was

purchased from AAPER, TX whereas propylene oxide (99%) was obtained from Sigma Aldrich, MO. Corn stover (average particle size 1.12 mm) was supplied by Idaho National Laboratory, ID. KOH (90%, Sigma Aldrich, MO), Pluronic F127 (BASF, TX) and HCl (35.5%, Fisher-Scientific, MA) were utilized for the synthesis of POC. All reagents were used as received.

### 2.2 Synthesis of ferrite and KOH-activated hydrochar electrode materials

Manganese (II) chloride tetrahydrate and iron (II) chloride tetrahydrate were taken in stochiometric proportion and dispersed in 30 mL of ethanol via sonication mixing. To the dispersion, 30 mL propylene oxide was added to accomplish the gel formation. The gel was aged for 24 hours and preheated to 120°C for 1 hour before subjected to calcination at 300°-900°C. The synthesis method for $MnFe_2O_4$ is schematically shown in Figure 1.

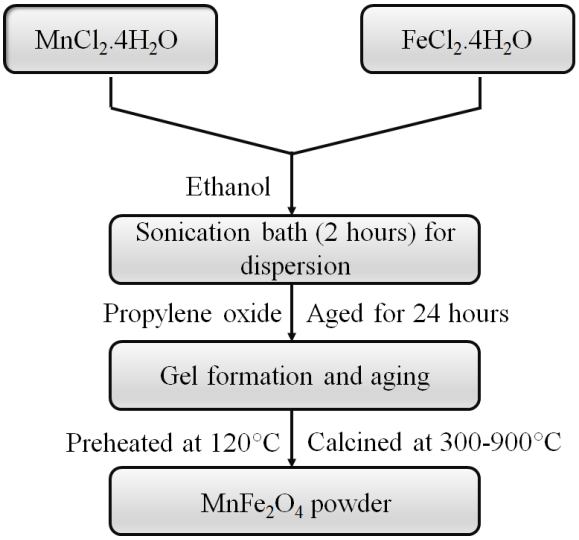


**Figure 1:** Sol-gel synthesis of $MnFe_2O_4$ electrode material.

To perform catalytic hydrothermal liquefaction (CHTL), corn stover and 5 wt.% $Ni(NO_3)_2$ catalyst were loaded in a PARR SS316 HTHP reactor (300 mL) at 250°C for 1 hour. After CHTL, the solid residue was filtered and washed with acetone to recover hydrochar and oil. The hydrochar was activated with KOH and thermally treated at 200°C under a constant flow of UHP $N_2$. Following thermal treatment, POC was acid washed with dilute HCl and dried at 60°C for 12 hours. Additional details for this methodology can be found elsewhere [11–15].

### 2.3 Characterization of Mn-ferrite

Phase composition of $MnFe_2O_4$ was studied using the Empyrean Series-3 powdered X-ray diffractometer. The diffractometer used a CoKα radiation (wavelength = 1.78899 Å) and operated at 45 kV, 40 mA. Powdered X-ray diffraction analysis was performed in $4° \leq 2\theta \leq 140°$ range, at the scan rate of 0.09° per second. Crystalline phases were determined using the MDI/JADE software.

### 2.4 Fabrication of ASC and electrochemical performance evaluation

Mn-ferrite and POC electrode materials were mixed with polyurethane and applied to two identical copper plates. With the electrode facing each other, a separator (Nylon 6,6) was dipped into aqueous KOH electrolyte and sandwiched between the copper plates. Entire assembly was sealed and taped with plastic film to avoid dust contamination. As fabricated ASCs were charged with 4 volts and 0.008 amps for 10 minutes. The performance of ASC was determined by Gamry G-300 potentiostat/galvanostat/ZRA instrument. Cyclic voltammetry tests were performed to determine the specific capacitance of ASCs. Additional details can be found elsewhere [12,16,17].

## 3 RESULTS AND DISCUSSION

The hydrochar yield after CHTL process, and POC characteristics such as specific surface area (SSA), pore size and pore volume are provided in Table 1.

**Table 1**: HTL-derived hydrochar yield and SSA, pore volume, pore size of KOH-activated hydrochar

| Hydrochar yield (%) | SSA ($m^2/g$) | Pore volume ($cm^3/g$) | Pore size range (nm) |
|---|---|---|---|
| 51-54 | 102 | 0.073 | 6.3-25 |

Powdered XRD pattern for the material calcined at 900°C is shown in Figure 2. The material was found to contain $Fe_2O_3$ (hematite) and $MnFe_2O_4$ crystalline phases at 8.96% and 91.04%, respectively. The $MnFe_2O_4$ phase in the sample matched with the 2-theta reflections reported by International Centre for Diffraction Data (ICDD).

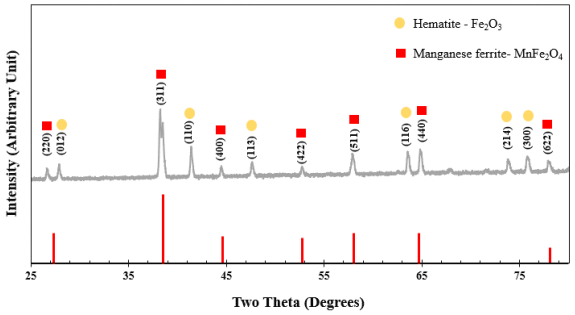


**Figure 2:** Powdered X-ray diffraction patterns of a) as-prepared $MnFe_2O_4$ calcined at 900°C, and b) reference peaks of $MnFe_2O_4$ as reported by ICDD

Figure 3 shows the KOH activated CHTL derived hydrochar, Mn-ferrite powder, and the schematic of ASC fabrication. Cyclic voltammetry (CV) plots were generated for the ASCs fabricated with $MnFe_2O_4$ at and POC electrodes. The CV measurements were performed with varying voltage window, which can be observed in Figure 4. At large voltage window and fast scan rate, the CV curves are observed to possess some distinct non-rectangular shapes, which are the characteristics of ASCs.

Powdered materials calcined at 300°, 600° and 900°C were used individually with POC material and ASCs were fabricated. CV measurements revealed specific capacitance of 4.2 – 64.7 F/g (Table 2). At 0.05 A/g current density, the specific capacitance of 64.7 F/g was observed for the ASC fabricated with $MnFe_2O_4$ calcined at 900°C and POC. The specific capacitance of 4.2 F/g and 27.6 F/g was observed for the ASCs fabricated with the powdered material calcined at 300°C and 600°C, respectively with POC electrode. It is believed that the presence of $MnFe_2O_4$ phase impacted the performance of ASCs.

The specific capacitance of the ASCs fabricated with Mn-ferrite is found to be lower as compared to the ASCs fabricated with (Mn, Ti)-mixed oxide electrode previously reported [11].

Currently, our group is investigating performance evaluation of the ASCs fabricated with different ferrites and POC electrode materials.

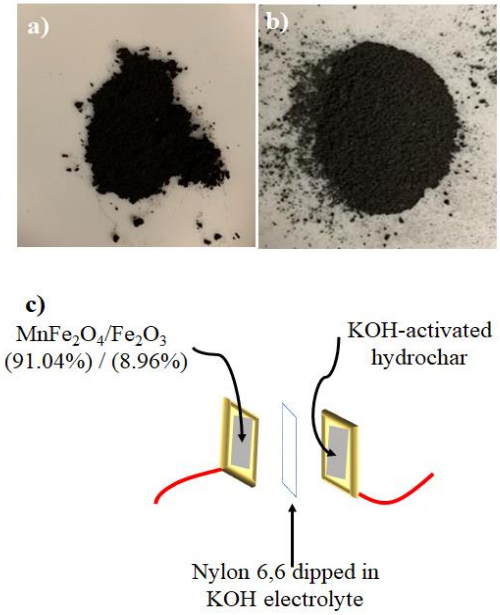


**Figure 3:** a) KOH activated CHTL derived hydrochar, b) Mn-ferrite calcined at 900°C and c) schematic of ASC fabricated with dissimilar electrodes.

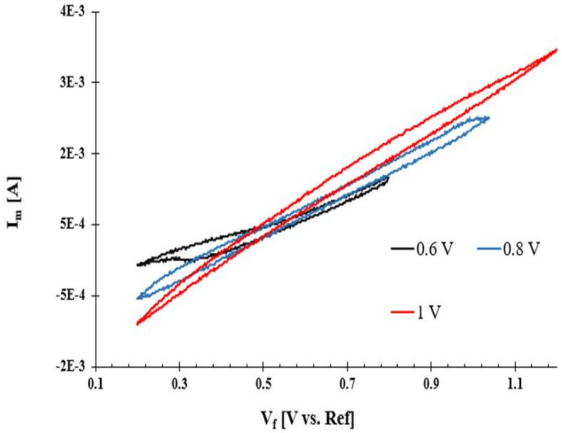


**Figure 4:** Cyclic voltammetry plots with varying voltage window for the ASC fabricated with $MnFe_2O_4$ and KOH activated CHTL derived hydrochar.

**Table 2:** Phase composition at different calcination temperatures, and the specific capacitance of ASCs fabricated with Mn-ferrite/char electrodes.

| Temp. (°C) | XRD phase | Electrodes for ASCs | Specific capacitance (F/g) |
|---|---|---|---|
| 300 | - | Mn/Fe oxide gel/char | 4.2 |
| 600 | - | | 27.6 |
| 900 | $MnFe_2O_4$ (91.04%) + $Fe_2O_3$ (8.96%) | | 64.7 |

## 4 CONCLUSION

Mn-ferrite was successfully synthesized by the sol-gel method followed by calcination at different temperatures. For the material calcined at 900°C, XRD pattern revealed the mixed phase containing $MnFe_2O_4$ and $Fe_2O_3$ at 91.04% and 8.96%, respectively. Using this electrode material as cathode with POC anode ASC was fabricated, which showed a specific capacitance of 64.7 F/g. Lower capacitance values were observed for the ASCs fabricated using the electrode materials calcined at 300º and 600ºC with POC.


## ACKNOWLEDGEMENTS

The authors thankfully acknowledge the financial support from US DOE/EERE-BETO DE-EE0008252, and Karen M. Swindler Department of Chemical and Biological Engineering.


## REFERENCES


[1] T.M. Gür, Energy & Environmental Science. 11, 2696–2767, 2018 https://doi.org/10.1039/C8EE01419A.

[2] W. Zhang, Y. Li, H. Kang, B. Yang, Z. Li, H. Liu, Electrochimica Acta. 404, 139725, 2022. https://doi.org/10.1016/j.electacta.2021.139725.

[3] N. Wu, X. Bai, D. Pan, B. Dong, R. Wei, N. Naik, R.R. Patil, Z. Guo, Advanced Materials Interfaces. 8, 2001710, 2021. https://doi.org/10.1002/admi.202001710.

[4] N. Choudhary, C. Li, J. Moore, N. Nagaiah, L. Zhai, Y. Jung, J. Thomas, Advanced Materials. 29, 1605336, 2017. https://doi.org/10.1002/adma.201605336.

[5] Z. Fang, M. Xu, Q. Li, M. Qi, T. Xu, Z. Niu, N. Qu, J. Gu, J. Wang, D. Wang, Over-Langmuir. 37, 2816–2825, 2021. https://doi.org/10.1021/acs.langmuir.0c03580.

[6] A.M. Patil, X. An, S. Li, X. Yue, X. Du, A. Yoshida, X. Hao, A. Abudula, G. Guan, Chemical Engineering Journal. 403, 126411, 2021. https://doi.org/10.1016/j.cej.2020.126411.

[7] V.S. Amar, J.A. Puszynski, R. V. Shende, Journal of Renewable and Sustainable Energy. 7, 023113, 2015. https://doi.org/10.1063/1.4915312.

[8] J.D. Houck, V.S. Amar, R. v. Shende, International Journal of Energy Research. 44, 12474-12484, 2020. https://doi.org/10.1002/er.5454.

[9] M.B. Askari, P. Salarizadeh, International Journal of Hydrogen Energy. 45, 27482–27491, 2020. https://doi.org/10.1016/j.ijhydene.2020.07.063.

[10] M. Fu, Z. Zhu, Q. Zhuang, Z. Zhang, W. Chen, Q. Liu, Ceramics International. 46, 28200–28205, 2020. https://doi.org/10.1016/j.ceramint.2020.07.319.

[11] K. Huynh, B. Maddipudi, V. Amar, J. Houck, R. Shende, HTL Derived Biochar for Supercapacitor Electrodes, in: TechConnect World Innovation Conference, TechConnect Briefs, 184-187, 2021.

[12] V.S. Amar, J.D. Houck, R. V. Shende, International Journal of Energy Research. 44 , 12546-12558, 2020. https://doi.org/10.1002/er.5938.

[13] K.M. Shell, V.S. Amar, J.A. Bobb, S. Hernandez, R. V. Shende, R.B. Gupta, Industrial & Engineering Chemistry Research. 61, 392–402, 2022. https://doi.org/10.1021/acs.iecr.1c03820.

[14] K.M. Shell, D.D. Rodene, V. Amar, A. Thakkar, B. Maddipudi, S. Kumar, R. Shende, R.B. Gupta, Bioresource Technology Reports. 13, 100625, 2021. https://doi.org/10.1016/j.biteb.2021.100625.

[15] V.S. Amar, J.D. Houck, B. Maddipudi, T.A. Penrod, K.M. Shell, A. Thakkar, A.R. Shende, S. Hernandez, S. Kumar, R.B. Gupta, R.V. Shende, Renewable Energy. 173, 329-341, 2021. https://doi.org/10.1016/j.renene.2021.03.126.

[16] J. Houck, V. Amar, R. Shende, Cobalt doped (Mn, Ti)-oxides for supercapacitors, in: TechConnect World Innovation Conference, TechConnect Briefs, 163-166, 2019.

[17] J. Houck, V. Amar, R. Shende, Mesoporous Nanocomposites of Mn and Ti Oxides for Supercapacitors, in: TechConnect World Innovation Conference, TechConnect Briefs, Materials for Energy, Efficiency and Sustainability: TechConnect Briefs 2018, 75-78, 2018.